# Casimir-Lifshitz Force based Optical Resonators

*Victoria Esteso[1], Sol Carretero-Palacios[1,2,]*, Hernán Míguez[1,]**

*1. Institute of Materials Science of Seville, Consejo Superior de Investigaciones Científicas (CSIC)- Univesidad de Sevilla (US). Américo Vespucio 49, 41092, Seville, Spain*

*2. Departamento de Física de Materiales, Universidad Autónoma de Madrid, 28049-Madrid, Spain*

**Corresponding Author**

h.miguez@csic.es, sol.carretero@uam.es

We theoretically investigate the building of optical resonators based on the levitation properties of thin films subjected to strong repulsive Casimir-Lifshitz forces when immersed in an adequate medium and confronted to a planar substrate. We propose a design in which cavities supporting high Q-factor optical modes at visible frequencies can be achieved by means of combining commonly found materials, such as silicon oxide, polystyrene or gold, with glycerol as a mediating medium. We use the balance between flotation and repulsive Casimir-Lifshitz forces in the system to accurately tune the optical cavity thickness and hence its modes. The effects of other forces, such as electrostatic, that may come into play are also considered. Our results constitute a proof of concept that may open the route to the design of photonic architectures in environments in which

dispersion forces play a substantial role, and could be of particular relevance for devising novel microfluidic optical resonators.

**TOC GRAPHICS**

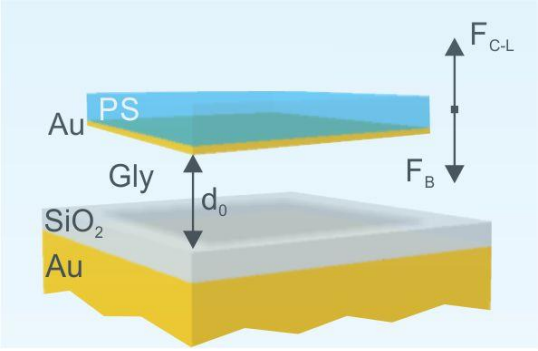


**KEYWORDS** Casimir-Lifshitz force, Optical resonator, Levitation, Plane-Parallel Plates

Very recently, repulsive Casimir-Lifshitz forces, $F_{(C-L)}$, have been demonstrated in metallic plates through an appropriate stratification of the inner dielectric media in a beautiful cutting-edge experiment.[1] In it, a gold nanoplate is submerged in ethanol in the vicinity of a Teflon-coated gold substrate. This scheme displays levitation due to the balance of buoyancy, $F_b$, and repulsive Casimir-Lifshitz forces, crowning the levitation phenomena previously proposed in literature,[2-6] and opening the path for a variety of applications such as contact-free nanomachines, ultrasensitive force sensors, and nanoscale manipulations based on such pursued repulsive dispersion force.[7-20]

Here, we further explore theoretically the possibility of building optical resonators supporting high Q-factor optical modes at visible frequencies formed by a bilayer metal plate in front of a planar substrate that levitates in a suitable liquid medium due to the balance of $F_b$ and repulsive $F_{(C-L)}$. The spectroscopic characterization of the optical resonator will yield the size of the cavity and, indirectly, the equilibrium distance at which the bilayer structure levitates. In an experiment based

on this approach in which quantum stable levitation is detected by spectroscopic techniques, and the equilibrium distance is quantified indirectly by measuring reflectance properties of the optical cavity formed by the facing metal plates, it is mandatory to have an excellent control on the measured layer thickness of all materials in the stratified cavity, and a perfect alignment between the parallel plates to accurately determine their spectral reflectance response and exclude dynamic situations out of equilibrium. In this context, the narrower the spectral features (provided by high Q-factor optical resonators), the better the precision of the geometrical parameters yielding the defined spectral response. In our design, optical resonators can be achieved by means of combining well-known materials, such as silicon dioxide ($SiO_2$), polystyrene (PS) and gold (Au), immersed in glycerol. Such solid materials present exceptional optical quality, and a fine tuning of their thicknesses is possible experimentally.[21,22] Additionally, in contrast to alcohols suffering from evaporation, glycerol presents stable dissipation properties with potential applications in promising technologies based on such levitation effect. In our approach, we use the balance between flotation and repulsive Casimir-Lifshitz forces acting on the system to accurately tune the optical cavity thickness and hence the modes in the devised optical resonator. The effects of other forces that may come into play, such as electrostatic ones, are also evaluated. Our results demonstrate a novel framework for the design and manipulation of photonic systems governed by dispersion forces.

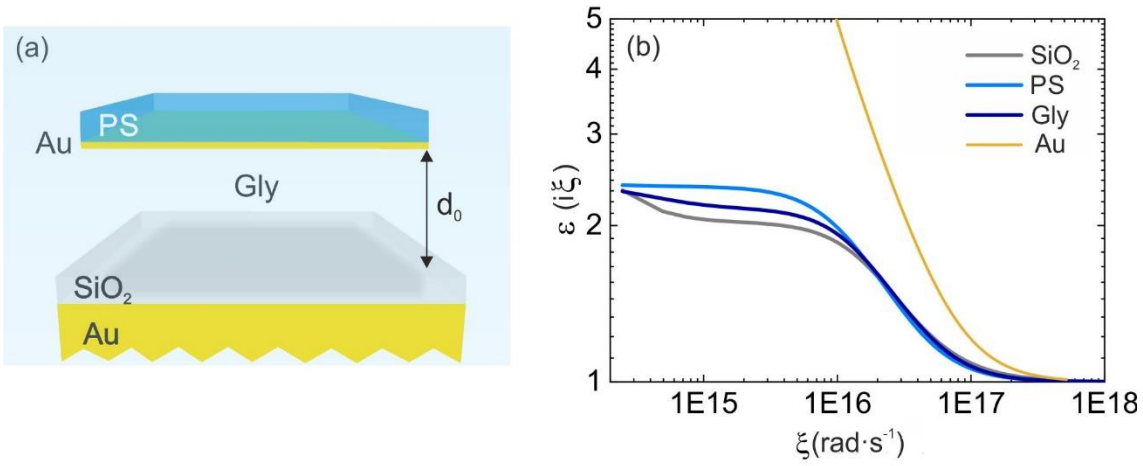


Figure 1: a) Scheme of the optical resonator proposed displaying levitation due to the balance of $F_{(C-L)}$ and $F_b$: it consists on a $SiO_2$-coated Au substrate with a suspended Au/PS bilayer on top. The whole arrangement is immersed in glycerol. Glycerol layer thickness between the substrate and the bilayer is denoted by $d_0$. In the case of levitation, $d_0 = d_{eq}$. b) Dielectric permittivities evaluated at Matsubara frequencies, $\varepsilon(i\xi_n)$, for the materials of choice: $SiO_2$ (in grey), PS (in blue), glycerol (in navy) and Au (in yellow).

A scheme of the proposed optical resonator is shown in **Figure 1**a. A Au substrate coated by a $SiO_2$ layer of variable thickness acts as one of the mirrors in the optical resonator design, on top of which the second mirror consisting on a golden PS bilayer of tunable thickness is immersed in glycerol at a separation distance $d_0$. Corresponding dielectric permittivities evaluated at Matsubara frequencies ($\varepsilon(i\xi_n)$), extracted from refs. [17,23-27], are shown in Figure 1b. The chosen materials are carefully selected, and they obey the following decisive conditions: i) their relative values of the imaginary part of the dielectric permittivities expressed in Matsubara frequencies fulfill the necessary inequation[7,11] to attain repulsive $F_{(C-L)}$, i.e., $\varepsilon^{SiO_2}(i\xi_n) < \varepsilon^{glycerol}(i\xi_n) < \varepsilon^{Au}(i\xi_n)$; ii) their density difference enables force balance and levitation at separation distances of hundreds of nanometers; and iii) their reflectivity in the visible spectral range is such that very fine spectral features impose high accuracy prediction on the gap distance in the optical resonator. Most

importantly, the design offers the possibility to tune one by one the effects on the interplay between $F_{(C-L)}$ and $F_b$ (despite these ones are intimately related through variations on the layers thicknesses). Roughly speaking, changes on the Au slab thickness of the suspended bilayer film will mainly modify the Q-factor of the optical resonator, whereas variations on the $SiO_2$ coating and PS film thicknesses will predominantly alter $F_{(C-L)}$ and $F_b$, respectively.

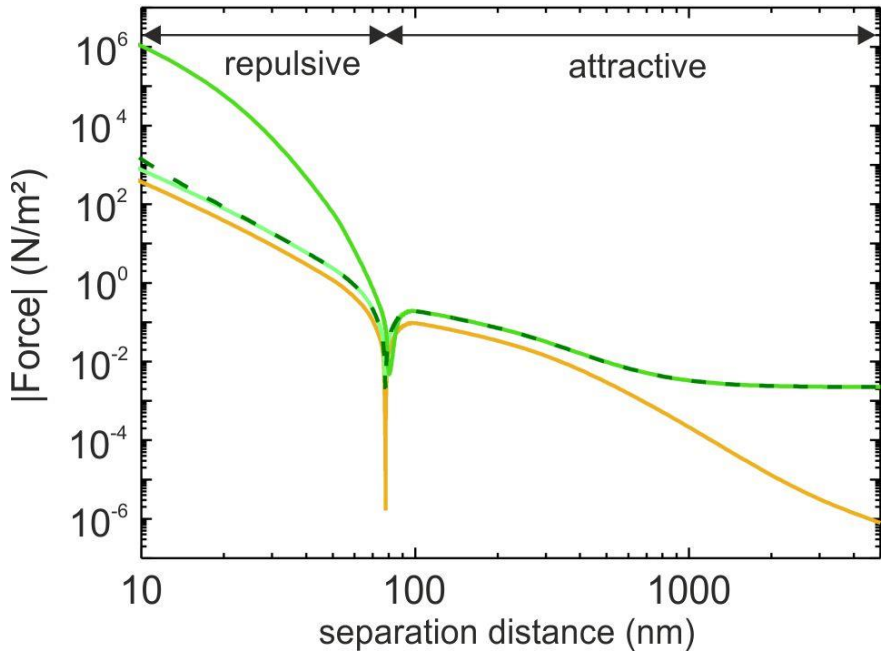


Figure 2: Modulus of the dominant forces (in logarithmic scale) acting on an exemplary levitating system (consisting on a 100 nm $SiO_2$ coating layer, and a Au/PS bilayer of 30 nm and 1500 nm thickness, respectively), as a function of the separation distance. $F_{(C-L)}$ is shown in yellow color, and $F_{(C-L)} + F_b + F_{el}$ assuming either $F_{el} = 0$ or the addition of a monovalent salt with concentrations 3 mM and 60 mM are shown in light green, dark green and dashed green colors, respectively.

Calculations of the dominant forces (in logarithmic scale) as a function of the separation distance between the $SiO_2$ coating and the suspended bilayer are shown in **Figure 2** for one exemplary optical resonator scheme. It consists on a $SiO_2$ coating of $d_{SiO_2} = 100$ nm, and a levitating Au/PS bilayer of $d_{PS} = 1500$ nm and $d_{Au} = 30$ nm thickness, respectively, immersed in glycerol. The

modulus of $F_{(C-L)}$ is depicted in yellow color. Also, the modulus of $F_{(C-L)} + F_b + F_{el}$ is shown in the same graph, taking either $F_{el} = 0$ (in light green) or the effect of repulsive electrostatic forces assuming a monovalent salt concentration of 3 mM (in dark green) or 60 mM (with dashed green line) dissolved in glycerol. Details of the force calculations, and the formalism employed,[7,28-31] are provided in the Supporting Information. The nature of the force (or sum of forces) changes with the separation distance from repulsive to attractive, and such a change is visible with an abrupt minimum in the figure, occurring at a separation distance $d_0 = d_{glycerol} \sim 80$ nm. This separation distance, in turn, corresponds to the equilibrium position, $d_{eq}$, at which the bilayer levitates. In this specific case, $d_{eq}$ is hardly modified by the presence of repulsive electrostatic forces. Nevertheless, at short separation distances, the addition of low salt concentrations in glycerol strengthens the repulsion between the metal plates, and its effect rapidly decays with the separation distance. In order to correlate levitation phenomena in our optical resonators to just the action of repulsive Casimir-Lifshitz forces balanced by buoyancy, in what follows we will assume that glycerol contains a high enough salt concentration to neglect $F_{el}$.

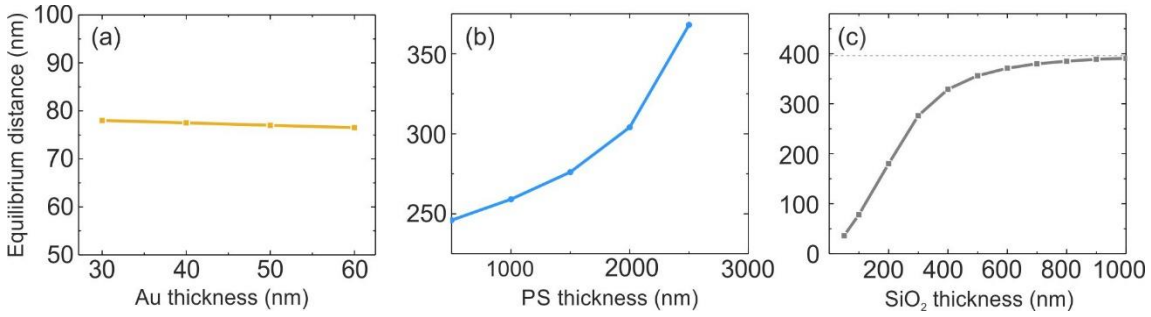


Figure 3: For diverse optical resonator designs, and assuming $F_{el} = 0$, equilibrium distance as a function of one of the slab thicknesses conforming the optical resonator arrangement: (a) for the Au layer (with $d_{SiO_2} = 100$ nm and $d_{PS} = 1500$ nm fixed) in the bilayer system, (b) the PS layer (with $d_{SiO_2} = 300$ nm and $d_{Au} = 30$ nm fixed), and (c) the $SiO_2$ coating layer (with $d_{PS} = 1500$ nm and $d_{Au} = 30$ nm fixed).

The equilibrium distance of the suspended Au/PS bilayer will depend upon the balance of $F_{(C-L)}$ and $F_b$ (since we are assuming $F_{el} = 0$), determined by the film thickness relation of the constitutive layers in the stratified system. **Figure 3** displays $d_{eq}$ as a function of the thickness of one of the slabs building the optical resonator, corresponding to either the Au (panel a), and PS (panel b) slabs in the bilayer arrangement, or the $SiO_2$ coating (panel c). For diverse illustrative optical resonator configurations experimentally doable (as specified in the figure caption), a wide range of nanoscale stable quantum trapping distances ($d_{eq} \in [40 – 400]$ nm) can be achieved. Specifically, steady $d_{eq}$ values around 75 nm are attained for all Au slab thicknesses considered (thicker slabs display gold bulk reflectance spectra, impeding the identification of the optical resonator), whereas these can be finely tuned within $d_{eq} \in [250 – 375]$ nm by enhancing $F_b$ with the PS thickness. Finally, we find that the film thickness of the $SiO_2$ coating strongly modulates $F_{(C-L)}$, broadening the $d_{eq}$ values range that could be attained. For thick enough $SiO_2$ slab thicknesses ($d_{SiO_2} > 800$ nm), $d_{eq}$ asymptotically approaches that of a system having a semi-infinite $SiO_2$ substrate (neglecting the Au substrate below), which is depicted by a horizontal dashed grey line in the figure.

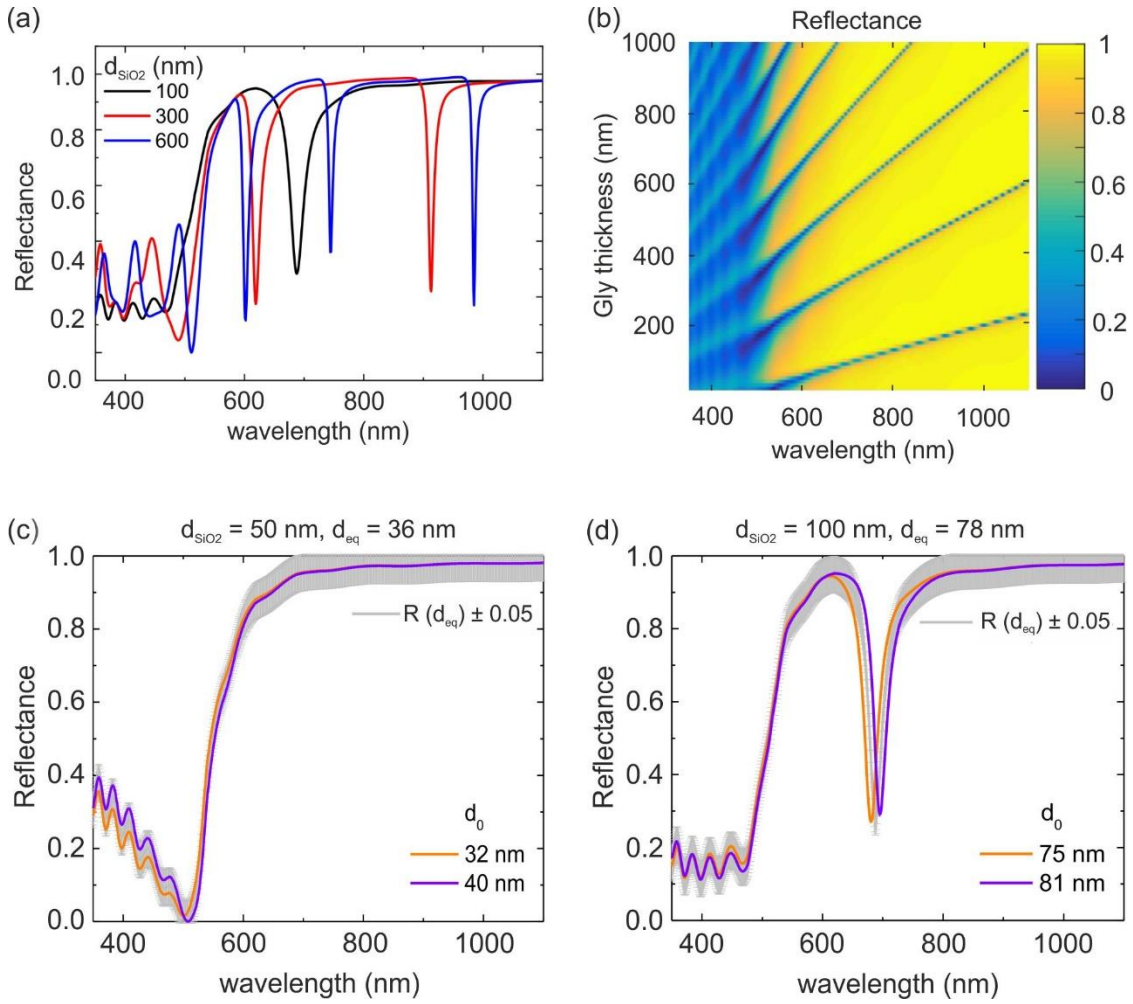


Figure 4: Reflectance spectra of several optical resonators. (a) Results for systems fixing $d_{PS}$ to 1500 nm, $d_{Au}$ to 30 nm, and considering variable $SiO_2$ coatings of 100 nm (in black), 300 nm (in red), and 600 nm (in blue) thickness, displaying stable quantum trapping at $d_{glycerol}$ = 78 nm, 276 nm, and 371 nm, respectively. (b) Reflectance contourplot as a function of the glycerol layer thickness between the immersed bilayer and the substrate, fixing $d_{PS}$ to 1500 nm, $d_{Au}$ to 30 nm and $d_{SiO_2}$ to 100 nm. Note that these results correspond to diverse optical resonators in which stable equilibrium only exists for one specific $d_{glycerol}$ thickness. (c) Results for a system displaying stable levitation corresponding to the set of parameters $d_{PS} = 1500$ nm, $d_{Au} = 30$ nm, $d_{glycerol} = d_{eq} = 36$ nm, and $d_{SiO_2} = 50$ nm, with an assumed error in the reflectance of ± 0.05 (in grey). For the same set of parameters, but separation distances $d_{glycerol} = d_0$ of 32 nm, and 40 nm, results are shown in orange and purple colors. These latter results would correspond to levitating systems out of equilibrium. (d) Results for the same set of parameters as in panel (c) yielding stable levitation, but considering $d_{SiO_2} = 100$ nm, thus, $d_{glycerol} = d_{eq} = 78$ nm, and assuming an error of ± 0.05 (in grey). Also, for separation distances of $d_{glycerol} = d_0$ of 75 nm, and 81 nm, results are shown in orange and purple colors. These latter results would correspond to levitating systems out of equilibrium.

The spectral optical reflectance in the visible frequency range of some exemplary optical resonator designs in which the levitating Au/PS bilayer parameters are fixed (defined in the figure caption), and the $SiO_2$ coating thickness is varied ($d_{SiO_2} = 100$ nm (in black), 300 nm (in red), and 600 nm (in blue)), are shown in **Figure 4**a. As previously mentioned, it is assumed $F_{el} = 0$ in all cases. Reflectance spectra are calculated employing the Transfer Matrix Method formalism.[32,33] All spectra display high reflectance bands over a wide spectral range, and very well defined minima at specific wavelengths, getting narrower and increasing in number with the Q-factor of the optical cavity, which varies from 25 to 164 as the cavity size increases (the cavity being formed by the $SiO_2$ coating layer and the glycerol film thickness). Such kind of well-defined spectral features allows an accurate prediction of the estimated equilibrium distance by indirect means. In Figure 4b, for a different set of fixed parameters (as indicated in the caption) and variable glycerol thicknesses, reflectance results are shown in a contourplot. Remarkably, the optical resonator design demonstrates that for $d_{glycerol}$ values as large as 1 μm, high Q-factor optical modes are sustained, providing distinct optical features resolved by univocal sets of geometrical parameters. Please bear in mind, on the one hand, that getting to stable levitation is a dynamic process in which levitation out of equilibrium can be observed, and on the other, that since all slab layers (except the glycerol one) are fixed to a certain thickness, only one of those spectra will correspond to a system displaying stable equilibrium, while the rest would correspond to levitating systems out of equilibrium. As it has been recently shown,[1] the optical features herein studied can be used to determine the separation distance between a levitating plate and a substrate interacting through repulsive Casimir-Lifshitz forces. Panels (c-d) demonstrate the need of having high Q-factor optical mode resonators to accurately determine this stable levitation position by means of spectroscopic techniques, and thus, the indirect measurement of $F_{(C-L)}$. For two $SiO_2$ coating

thicknesses, 50 nm (c) and 100 nm (d), reflectance spectra of levitating films are shown in grey color. A deviation of ± 0.05 in the reflectance response arising from the aforementioned error sources (misalignment, surface roughness, neglected electrostatic forces, layer thickness precision…) is also assumed. Reflectance spectra of the same system out of equilibrium are additionally shown. In particular, for thin $SiO_2$ coating thicknesses (panel c), reflectance spectra of systems located at $d_0$ = 32 nm, and 40 nm, fall within the estimated ± 0.05 reflectance error. This means that in a possible experiment based on this approach, any measured distance within the range $d_0 \in$ [32-40] nm could be inaccurately correlated to stable levitation arising from just the balance of Casimir-Lifshitz forces and buoyancy, neglecting the possible presence of additional forces (such as electrostatic ones) or disregarding the experimental tolerance. However, a design displaying high-Q factor optical modes as the one devised in panel (d), can unambiguously determine the stable levitating position. Remarkably, the well-defined spectral minimum corresponds to a unique set of parameters, corroborated by the fact that, reflectance spectra of systems out of equilibrium at $d_0$ = 75 nm, and 81 nm (a 6 nm distance range, like the one considered in panel (c)) lie outside the assumed ± 0.05 error in the reflectance spectrum. It is thus clear that the narrower the spectral features (provided by high Q-factor optical resonators), the better the precision of the geometrical parameters yielding the defined spectral response.

To conclude, we have shown the possibilities of building optical resonators supporting high Q-factor optical modes to indirectly determine unambiguously, by spectroscopic techniques, the stable equilibrium position at which a suspended bilayer levitates over a planar substrate due to the balance of repulsive Casimir-Lifshitz forces and buoyancy. Materials building the optical resonator are, specifically, $SiO_2$, PS, Au and glycerol, which are carefully selected as they display pivotal characteristics, such as repulsive Casimir-Lifshitz forces, densities providing buoyancy

capable to balance such dispersion force at measurable nanoscale distances, high optical quality and easy experimental fabrication. Moreover, glycerol presents stable properties in comparison to alcohols suffering from evaporation. We have demonstrated that stable quantum trapping distances covering a wide range ($d_{eq} \in [40 – 400]$ nm) can be applied by varying the film thickness of the materials involved. Finally, we have shown the need of building high Q-factor optical resonators to uniquely determine the stable equilibrium position and corresponding Casimir-Lifshitz force acting on the system, as associated errors in the dynamic experimental procedure could potentially yield wrong estimations of the levitation phenomena.

ASSOCIATED CONTENT

**Supporting Information**. Details of the theoretical formalism employed to calculate the total force acting on the suspended bilayer system, i.e., Casimir-Lifshizt force, buoyancy and electrostatic force.

AUTHOR INFORMATION

**Corresponding Author**

h.miguez@csic.es, sol.carretero@uam.es

**ORCID**

Victoria Esteso: 0000-0002-1976-8306

Sol Carretero-Palacios: 0000-0001-9915-5050

Hernán Míguez: 0000-0003-2925-6360

**Notes**

The authors declare no competing financial interests.

ACKNOWLEDGMENT

We acknowledge support from the Spanish Ministry of Science, Innovation and Universities for funding under grant EXPLORA FIS2017-91018-EXP. S.C.-P. acknowledges for funding through a Juan de la Cierva Incorporación under grant IJCI-2016-28549. The project that gave rise to these results received the support of a fellowship granted to V.E. from "la Caixa" Foundation (ID 100010434). The fellowship code is LCF/BQ/ES15/10360025.

REFERENCES

(1) Zhao, R.; Li, L.; Yang, S.; Bao, W.; Xia, Y.; Ashby, P.; Wang, Y.; Zhang, X. Stable Casimir Equilibria and Quantum Trapping. *Science* **2019**, *364* (6444), 984–987. https://doi.org/10.1126/science.aax0916.

(2) Rodriguez, A. W.; Munday, J. N.; Joannopoulos, J. D.; Capasso, F.; Dalvit, D. A. R.; Johnson, S. G. Stable Suspension and Dispersion-Induced Transitions from Repulsive Casimir Forces between Fluid-Separated Eccentric Cylinders. *Phys. Rev. Lett.* **2008**, *101* (19). https://doi.org/10.1103/PhysRevLett.101.190404.

(3) Esteso, V.; Carretero-Palacios, S.; Míguez, H. Effect of Temperature Variations on Equilibrium Distances in Levitating Parallel Dielectric Plates Interacting through Casimir Forces. *J. Appl. Phys.* **2016**, *119* (14). https://doi.org/10.1063/1.4945428.

(4) Esteso, V.; Carretero-Palacios, S.; Míguez, H. Nanolevitation Phenomena in Real Plane-Parallel Systems Due to the Balance between Casimir and Gravity Forces. *J. Phys. Chem. C* **2015**, *119* (10), 5663–5670. https://doi.org/10.1021/jp511851z.

(5) Rodriguez, A. W.; McCauley, A. P.; Woolf, D.; Capasso, F.; Joannopoulos, J. D.; Johnson, S. G. Nontouching Nanoparticle Diclusters Bound by Repulsive and Attractive Casimir Forces. *Phys. Rev. Lett.* **2010**, *104* (16). https://doi.org/10.1103/PhysRevLett.104.160402.

(6) Rahi, S. J.; Zaheer, S. Stable Levitation and Alignment of Compact Objects by Casimir

Spring Forces. *Phys. Rev. Lett.* **2010**, *104* (7). https://doi.org/10.1103/PhysRevLett.104.070405.

(7) Dzyaloshinskii, I. E.; Lifshitz, E. M.; Pitaevskii, L. P. General Theory of van Der Waals' Forces. *Uspekhi Fiz. Nauk* **2014**, *73* (3), 381–422. https://doi.org/10.3367/ufnr.0073.196103b.0381.

(8) Ninham, B. W.; Parsegian, V. A. Van Der Waals Forces: Special Characteristics in Lipid-Water Systems and a General Method of Calculation Based on the Lifshitz Theory. *Biophys. J.* **1970**, *10* (7), 646–663. https://doi.org/10.1016/S0006-3495(70)86326-3.

(9) Richmond, P.; Ninham, B. W. Calculations, Using Lifshitz Theory, of the Height vs. Thickness for Vertical Liquid Helium Films. *Solid State Commun.* **1971**, *9* (13), 1045–1047. https://doi.org/10.1016/0038-1098(71)90459-5.

(10) Milton, K. A. The Casimir Effect: Recent Controversies and Progress. *J. Phys. A. Math. Gen.* **2004**, *37* (38). https://doi.org/10.1088/0305-4470/37/38/R01.

(11) Munday, J. N.; Capasso, F.; Parsegian, V. A. Measured Long-Range Repulsive Casimir-Lifshitz Forces. *Nature* **2009**, *457* (7226), 170–173. https://doi.org/10.1038/nature07610.

(12) Lamoreaux, S. K. The Casimir Force: Background, Experiments, and Applications. *Reports on Progress in Physics*. January 2005, pp 201–236. https://doi.org/10.1088/0034-4885/68/1/R04.

(13) Bostrom, M.; Sernelius, B. Thermal Effects on the Casimir Force in the 0.1- 5 &mgr;m Range. *Phys. Rev. Lett.* **2000**, *84* (20), 4757–4760. https://doi.org/10.1103/PhysRevLett.84.4757.

(14) Bentsen, V. S.; Herikstad, R.; Skriudalen, S.; Brevik, I.; Høye, J. S. Calculation of the Casimir Force between Similar and Dissimilar Metal Plates at Finite Temperature. *J. Phys.*

*A. Math. Gen.* **2005**, *38* (43), 9575–9588. https://doi.org/10.1088/0305-4470/38/43/011.

(15) Yampol'skii, V. A.; Savel'Ev, S.; Mayselis, Z. A.; Apostolov, S. S.; Nori, F. Anomalous Temperature Dependence of the Casimir Force for Thin Metal Films. *Phys. Rev. Lett.* **2008**, *101* (9). https://doi.org/10.1103/PhysRevLett.101.096803.

(16) Obrecht, J. M.; Wild, R. J.; Antezza, M.; Pitaevskii, L. P.; Stringari, S.; Cornell, E. A. Measurement of the Temperature Dependence of the Casimir-Polder Force. *Phys. Rev. Lett.* **2007**, *98* (6). https://doi.org/10.1103/PhysRevLett.98.063201.

(17) Van Zwol, P. J.; Palasantzas, G. Repulsive Casimir Forces between Solid Materials with High-Refractive-Index Intervening Liquids. *Phys. Rev. A - At. Mol. Opt. Phys.* **2010**, *81* (6). https://doi.org/10.1103/PhysRevA.81.062502.

(18) Milling, A.; Mulvaney, P.; Larson, I. Direct Measurement of Repulsive van Der Waals Interactions Using an Atomic Force Microscope. *J. Colloid Interface Sci.* **1996**, *180* (2), 460–465. https://doi.org/10.1006/jcis.1996.0326.

(19) Lee, S. woo; Sigmund, W. M. AFM Study of Repulsive van Der Waals Forces between Teflon AF$^{TM}$ Thin Film and Silica or Alumina. *Colloids Surfaces A Physicochem. Eng. Asp.* **2002**, *204* (1–3), 43–50. https://doi.org/10.1016/S0927-7757(01)01118-9.

(20) Feiler, A. A.; Bergström, L.; Rutland, M. W. Superlubricity Using Repulsive van Der Waals Forces. *Langmuir* **2008**, *24* (6), 2274–2276. https://doi.org/10.1021/la7036907.

(21) Huang, J.; Juszkiewicz, M.; De Jeu, W. H.; Cerda, E.; Emrick, T.; Menon, N.; Russell, T. P. Capillary Wrinkling of Floating Thin Polymer Films. *Science* **2007**, *317* (5838), 650–653. https://doi.org/10.1126/science.1144616.

(22) Cerqua, K. A.; Hayden, J. E.; LaCourse, W. C. Stress Measurements in Sol-Gel Films. *J. Non. Cryst. Solids* **1988**, *100* (1–3), 471–478. https://doi.org/10.1016/0022-3093(88)90066-

X.

(23) Kitamura, R.; Pilon, L.; Jonasz, M. Optical Constants of Silica Glass from Extreme Ultraviolet to Far Infrared at near Room Temperature. *Appl. Opt.* **2007**, *46* (33), 8118. https://doi.org/10.1364/AO.46.008118.

(24) Hsu, H. S.; Chien, P. C.; Sun, S. J.; Chang, Y. Y.; Lee, C. H. Room Temperature Ferromagnetism in Co-Doped Amorphous Carbon Composites from the Spin Polarized Semiconductor Band. *Appl. Phys. Lett.* **2014**, *105* (5). https://doi.org/10.1063/1.4892561.

(25) Inagaki, T.; Arakawa, E. T.; Hamm, R. N.; Williams, M. W. Optical Properties of Polystyrene from the Near-Infrared to the x-Ray Region and Convergence of Optical Sum Rules. *Phys. Rev. B* **1977**, *15* (6), 3243–3253. https://doi.org/10.1103/PhysRevB.15.3243.

(26) Folks, W. R.; Pandey, S. K.; Pribil, G.; Slafer, D.; Manning, M.; Boreman, G. Reflective Infrared Ellipsometry of Plastic Films. *Int. J. Infrared Millimeter Waves* **2006**, *27* (11), 1553–1571. https://doi.org/10.1007/s10762-006-9150-3.

(27) Svetovoy, V. B.; Van Zwol, P. J.; Palasantzas, G.; De Hosson, J. T. M. Optical Properties of Gold Films and the Casimir Force. *Phys. Rev. B - Condens. Matter Mater. Phys.* **2008**, *77* (3). https://doi.org/10.1103/PhysRevB.77.035439.

(28) Casimir, H. B. . On the Attraction Between Two Perfectly Conducting Plates. *Indag. Math* **1948**, *10*, 261–263.

(29) Lifshitz, E. M. The Theory of Molecular Attractive Forces between Solids. *J. Exp. Theor. Phys.* **1955**, *29* (1), 94–110.

(30) Cappella, B.; Dietler, G. Force-Distance Curves by Atomic Force Microscopy. *Surf. Sci. Rep.* **1999**. https://doi.org/10.1016/S0167-5729(99)00003-5.

(31) Parsegian, V. A.; Gingell, D. On the Electrostatic Interaction across a Salt Solution between

Two Bodies Bearing Unequal Charges. *Biophys. J.* **1972**. https://doi.org/10.1016/S0006-3495(72)86155-1.

(32) Thompson, R. C. Optical Waves in Layered Media. *J. Mod. Opt.* **1990**. https://doi.org/10.1080/09500349014550171.

(33) Hecht, E. Hecht Optics. *Addison Wesley* **1998**.